Planar Wide Mesh Scanning using Multi-Probe Systems

Fernando Rodríguez Varela(1), Manuel Sierra Castañer(2), Francesco Saccardi(3), Lucia Scialacqua(3), Lars Foged(3)

(1) Microwave Engineering and Radiocommunication Systems Group, Universidad Rey Juan Carlos de Madrid, Spain
(2) Information Processing and Telecommunications Center, Universidad Politécnica de Madrid, Spain
(3) Microwave Vision Group, Italy
fernando.varela@urjc.es, manuel.sierra@upm.es, lars.foged@mvg-world.com

***Abstract*—The reduction of acquisition time in planar near field systems is a high interest topic when active arrays or multi beam antennas are measured. Different solutions have been provided in the last years: multi-probe measurements systems and the Planar Wide Mesh (PWM) methodology, which implements a non redundant sampling scheme that reduces the number of samples required for the far-field transformation, are two of the most well known techniques. This paper proposes the combination of both approaches to derive a multi-probe PWM grid which reduces the measurement times to the minimum. The method is based on treating the near-field to far-field transformation as an inverse source problem. The multi probe PWM is designed with a global optimization process which finds the best measurement locations of the probe array that guarantee a numerically stable inversion of the problem. A simulated measurement example with the VAST12 antenna is presented where the total number of samples is reduced by a factor of 100 using a 4×4 probe array.**

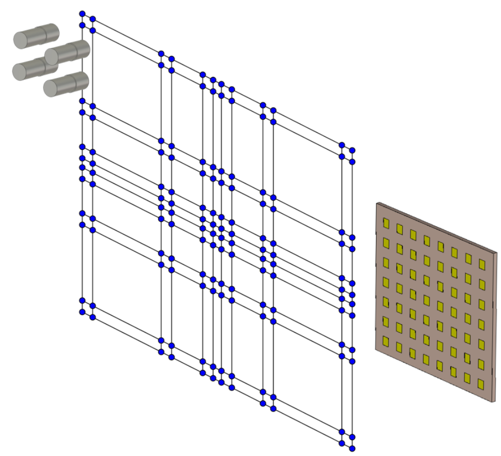

Fig. 1. Planar Wide Mesh measured by a 2×2 probe array.

I. Introduction

Planar near-field measurements (PNF) [1]-[3] are a popular alternative for large antenna testing. In this methodology the antenna under test (AUT) is kept stationary and the radiated field is scanned with the probe on a planar regular grid. This leads to a very simple mechanical process, in contrast to more complex techniques like CATR [4] or spherical near-field testing [5]. Furthermore, when testing very directive antennas pointing at boresight, the sampling step and scan truncation can be relaxed achieving high reductions of measurement time.

Nevertheless, in some cases it is necessary to perform measurements in large scanning planes with $\lambda/2$ sampling step. This is the case of low directive AUTs where the near-field is spread over a large plane, but also directive antennas with steered beams like phased arrays. This may raise the measurement times to the order of several hours per AUT, leading to a bottleneck in the antenna development and testing process. Thus, more advanced techniques must be derived to reduce the measurement times.

The most straightforward way to do so is the use of multi-probe systems [6]-[8], so several measurements can be performed at the same time with the help of switches or multiple receivers. A common implementation is the arrangement of several probes over a column array which reduces the mechanical movement of the probe over the vertical dimension. On the horizontal dimension the scanning is performed moving the probe array as in a conventional single probe measurement.

An alternative approach is the use of advanced post processing algorithms that reduce the number of samples required for the near-field to far-field transformation. After a rigorous study on the spatial bandwidth of electromagnetic fields [9][10] it is possible to design a minimum redundancy planar grid, which captures all information about the AUT. Such grid is called Planar Wide Mesh (PWM) [11]-[13]. The PWM exhibits a high density sampling in the regions close to the aperture and then it decreases gradually as the probe gets far from the AUT.

This paper proposes the combination of multi-probe systems with the concepts of PWM to minimize the measurement time of large AUT and plane near-field measurements. The far-field transformation will be formulated as an inverse problem, being the AUT aperture fields the unknowns to be solved. The success on solving this problem depends on its condition number, which can be assessed with Singular Value Decomposition (SVD) techniques [14]-[18]. A global optimization is performed to find the measurement grid that maximizes the condition number with the minimum number of samples. The optimizer is constrained to find solutions which are compatible with the geometry of the multi-probe system.

II. Theoretical background

A. Matrix problem formulation

An aperture antenna is considered in the center of the XY plane of a spherical coordinate system. The field radiated by the antenna on the $z > 0$ space admits an expansion in terms of Plane Wave Spectrum (PWS):

$$\vec{P}\left(k_x, k_y\right) = \int_{-\infty}^{\infty}\int_{-\infty}^{\infty} \vec{E}(x, y) e^{-j(k_x x + k_y y)} dx dy \quad (1)$$

being $\vec{E}$ the aperture field and $\vec{P}$ its PWS. The latter can be used to compute the signal received by a probe on any point $\vec{r} = (x, y, z)$ of the $z > 0$ subspace:

$$b_{probe}(\vec{r}) = \int_{-\infty}^{\infty}\int_{-\infty}^{\infty} \vec{S}\left(k_x, k_y\right) \cdot \vec{P}\left(k_x, k_y\right) e^{j\vec{k}\cdot\vec{r}} dk_x dk_y \quad (2)$$

being $\vec{k}$ the vector wave number (k_x, k_y, k_z) and $\vec{S}$ the probe spectrum.

In conventional planar near-field measurements, b_{probe} is measured on a $z = z_0$ plane and the AUT pattern is found by inverting (2). In this paper we take a different approach by defining the discretized matrix representation of (1-2):

$$\boldsymbol{p} = \boldsymbol{C_1 e_{aper}} \quad (3)$$

$$\boldsymbol{b_{probe}} = \boldsymbol{C_2 p} \quad (4)$$

where $\boldsymbol{p}$, $\boldsymbol{b_{probe}}$ and $\boldsymbol{e_{aper}}$ are column vectors containing the samples of the PWS, measured plane and aperture fields, respectively. $\boldsymbol{C_1}$ and $\boldsymbol{C_2}$ are the radiation matrices performing the Fourier integrals in (1) and (2) respectively. Eqs (3-4) can be combined to relate directly the field on tha aperture to that in the measured plane:

$$\boldsymbol{e_{meas}} = \boldsymbol{C_2 C_1 e_{aper}} \quad (5)$$

Eq. 5 forms a system of equations that can be solved to retrieve the aperture fields from the knowledge of the planar near-field measurements. In a second step, the AUT PWS is obtained using (3), which gives the radiation pattern of the antenna.

B. Inversion problem using Truncated SVD

The number of equations in (5) is equal to the number of near-field samples of the measurement. On the other hand, the number of samples in the AUT aperture is a parameter that must be adjusted. If a high value is chosen, we obtain a detailed representation of $\vec{E}$ at the cost of increasing the number of unknowns. Thus, there exist a trade off between the proper representation of the aperture field and the numerical stability of the system of equations.

A truncated SVD approach helps to balance this trade-off. The SVD expansion of matrix $\boldsymbol{C} = \boldsymbol{C_2 C_1}$ quantifies the contribution of all aperture samples to the radiation on the plane on the antenna. Therefore it is possible to eliminate those unknowns which do not contribute significantly using a reduced-order model of (5) [14]:

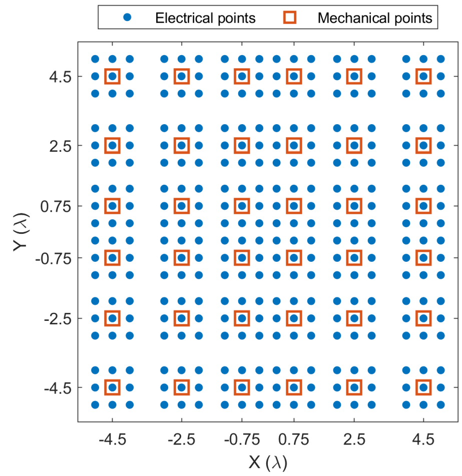

Fig. 2. Example of PWM illustrating the concept of mechanical and electrical measurement points

$$\boldsymbol{b_{probe}} = \boldsymbol{C_t e_{ap,t}} \quad (6)$$

being $\boldsymbol{C_t}$ and $\boldsymbol{e_{ap,t}}$ the truncated versions of $\boldsymbol{C}$ and $\boldsymbol{e_{ap}}$ respectively. Now this problem can be solved accurately by a matrix inversion in a linear squares sense. Because the SVD analysis only depends on the system matrix, these results are independent of the aperture field specific distribution.

C. Optimization of the measurement locations

The success on solving (6) depends on the location of the measurement samples. The goal is to design a measurement grid that captures all the degrees of freedom of the aperture field. This can be done by analyzing the condition number of $\boldsymbol{C_t}$ [15][19]. A low condition number means an accurate reconstruction of $\boldsymbol{e_{ap,t}}$, which means low radiation pattern uncertainties.

A global optimization algorithm is proposed to select the best measurement points. To simplify the formulation, a square symmetric mesh with equal rows and columns is considered. This means we only need to optimize the location of the multi-probe array over one dimension and then generalize it to the plane. Such simplification reduces drastically the number of optimization variables.

As an example, a MP system of 3×3 probes is considered. This probe array is scanned in a grid of 6×6 "mechanical points", leading to a total of 18×18 "electrical points". The resulting grid is depicted in Fig. 2. Due to the symmetry considerations we have assumed, the complete grid is defined by 3 "control points" which are $(0.75\lambda, 2.5\lambda, 4.5\lambda)$.

The coordinates of the mesh control points are found by a particle swarm optimization with the following parameters:

- Optimization variable: vector of Nc mesh control points.
- Objective function fitness: condition number of the system matrix C_t.

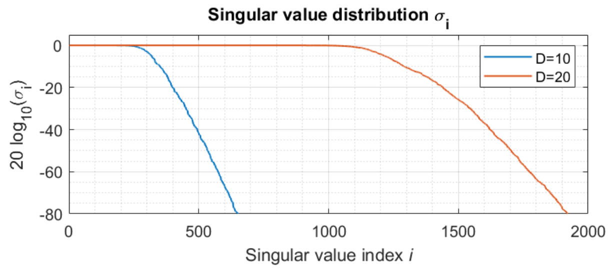

Fig. 3. Singular value distribution of $\boldsymbol{C}$ for several AUT aperture sizes

- Auxiliary parameters: number of probes along each dimension N_p, probe separation Δ_p, AUT aperture dimension, frequency and measurement distance.

The value of Nc is yet to be defined. This parameter regulates the total number of field samples in the grid so it is critical for the system conditioning. There are no rules for setting this parameter, so the optimal value is found by performing sequential optimizations for different values. Low values of Nc will yield too coarse grids with poor condition numbers. As soon as we start increasing Nc the optimizer will be able to design grids with better conditioning. This process stops when the condition number reaches an acceptable value, e.g. 10^4. In conclusion, this procedure finds the optimal grid with the minimun number of samples that ensure a stable matrix inversion.

III. Numerical discussion

In this section we asses the feasibility of the proposed technique in large AUTs using a common MVG multi-probe module working in the 8-18 GHz band [20]. A planar near-field measurement scenario is simulated with the following parameters:

- AUT: $D \times D$ aperture.
- Target validity angle: 70º.
- $N_p \times N_p$ square array of probes with $\Delta_p = 10$ cm.
- Measurement distance $z_0 = 8\lambda$.

Two different values of D will be used to assess the influence of the AUT size in the design of the multi-probe PWM grid. The first step is the identification of the number of significant singular values of each aperture. Fig. 3 shows the singular values of matrix $\boldsymbol{C}$. For $D = 10\lambda$, the power drops below -60 dB for a singular value index of 580. In other words, 580 samples are sufficient to represent the aperture field with a -60 dB accuracy. For the case of $D = 20\lambda$ this number increases to 1800 because the aperture has more degrees of freedom.

Once the truncation index for the aperture fields has been selected, the next step is the optimization of the mechanical point coordinates. This process has been performed for several frequencies and values of N_p ranging from 4 to 8. Fig. 4 depicts the number of mechanical points on each dimension of the optimized grids. For example, in the case of $D = 20\lambda$ at 18 GHz, a 4×4 probe array requires a grid of 13×13 mechanical points. For $D = 10\lambda$ a 9×9 grid is sufficient for a stable matrix inversion because the number of unknowns is also lower.

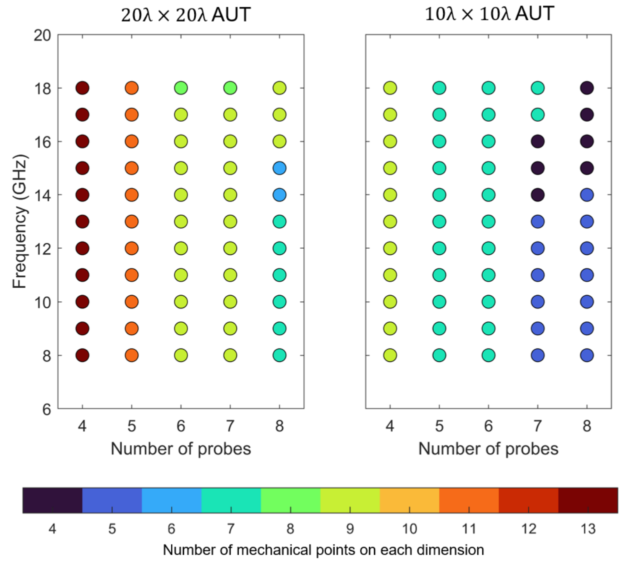

Fig. 4. Number of mechanical pints of the PWM for several probe arrays.

The relationship between number of mechanical points and aperture size is not linear, because the values of N_p and Δ_p highly influence the performance of the optimization algorithm. In general the optimization works best for low values of N_p. High values of this parameter lead to more redundant grids which compromise the measurement time reductions. Therefore, it is more convenient to arrange the arrays is square patterns so the probes are distributed over both vertical and horizontal axis.

IV. Antenna measurement example

This section demonstrates the potential of the multi-probe PWM approach for measurement of real antennas. At the time of the measurements the proposed probe array was not available, so a combination of measurements and simulations has been performed instead.

The selected AUT is the Validation Standard antenna (VAST12) [21], a 50 cm diameter offset reflector with astigmatism, which produces a non conventional radiation pattern very convenient for inter comparison-campaigns [22]. The AUT was measured at 12 GHz in a spherical near-field system and its PWS is computed using the *SWEtoPWE* transformation [23][24].

The PWS is used to simulate two PNF measurements in a 90×90 cm^2 plane at a distance of 20 cm with a WR90 open-ended waveguide. This yields a validity angle of around 70º. Additive White Gaussian Noise of is added to simulate a finite dynamic range of -50 dB. The first PNF is simulated with a uniform $\lambda/2$ (1.25 cm) sampling step in both dimensions to emulate a conventional measurement. The second PNF is simulated in a PWM grid that is optimized as follows.

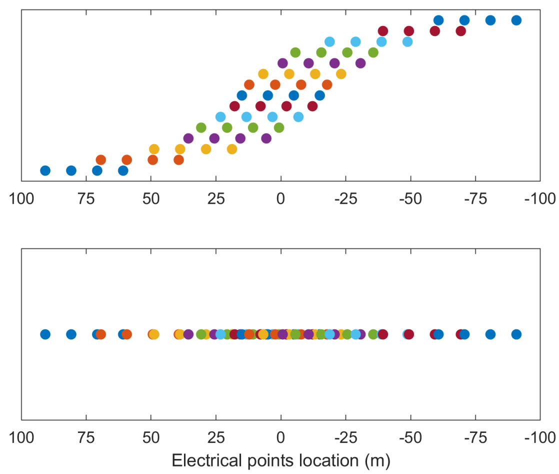

Fig. 5. Electrical points coordinates in a line of the optimized PWM (bottom) and its exploded view (top).

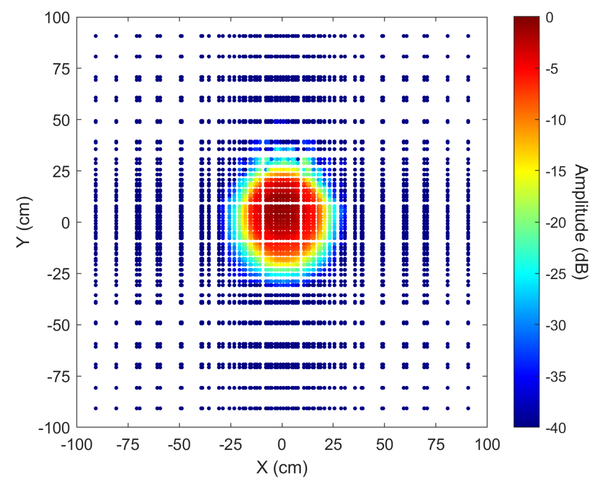

Fig. 6. Electrical points coordinates of the optimized PWM and near-field.

First, matrix $\boldsymbol{C}$ is built according to the aperture dimensions of the AUT. Secondly, $\boldsymbol{C}$ is truncated to a singular value level of -60 dB. The resulting matrix $\boldsymbol{C_t}$ leads to an inversion problem of 1800 unknowns. The next step is the optimization of the probe array locations. A 4×4 array of probes separated 10 cm is used. The iterative optimization process is evaluated to find the minimum number of mechanical points that give a conditioning number lower than 10^4. This is achieved by 15 mechanical points, which amount to a total of 60 electrical points on each dimension. Fig. 5 shows the distribution of the electrical points. Since they tend to be concentrated around the origin, an exploded view of the points has also been added. Finally, the complete PWM grid is obtained replicating the point distribution of Fig. 5 in both dimensions. This has been depicted in Fig. 6, along with the amplitude of the near-field on the sampling points.

The two simulated PNF grids are postprocessed to retrieve the far-field of the AUT. The uniform sampling grid is processed with traditional PWS techniques, so it can be used as a reference for comparing the proposed method. Figs. 7 and 8 show the far-field E and H planes respectively. The agreement between both approaches is perfect for both CP and XP components, with error levels below the noise floor. This demonstrates the accuracy and numerical stability of the mesh designed by the global optimizer.

The potential reductions in measurement time of the proposed approach are remarkable. The conventional PNF grid has 148×148 points. The optimized PWM grid contains 60×60 electrical points, but only 15×15 mechanical points are needed thanks to the multi-probe scanning. This gives a reduction factor of around 10 times on each dimension, i.e. a total of reduction of 100 times for the full plane. The actual savings on measurement time will depend on the probe movement and switching speed and whether the samples are taken in step mode or on-the-fly.

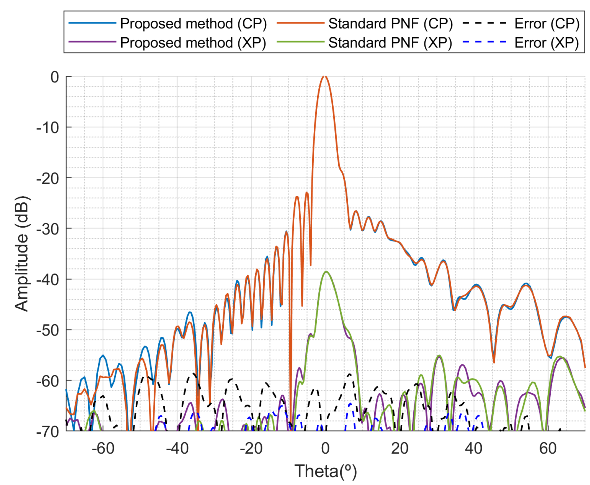

Fig. 7. VAST12 E-plane pattern comparison

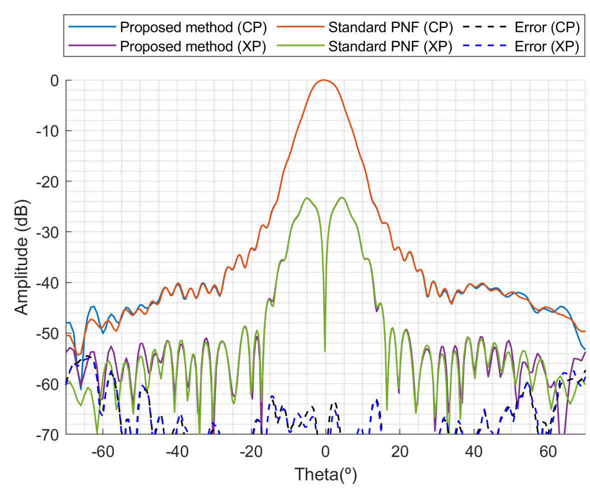

Fig. 8. VAST12 H-plane pattern comparison.

V. Conclusion

The capabilities of multi-probe arrays have been combined with the concept of Planar Wide Mesh scanning to develop a technique for fast antenna testing. The technique is based on solving the near-field to far-field transformation problem as a matrix inversion. The number of unknowns are minimized using truncated SVD methodology. Finally, the measurement point locations of the multi-probe array are obtained through a global optimization process where the fitness function is the condition number of the matrix to be inverted. The only a priori information required about the AUT is the physical extent of its aperture.

The feasibility of the proposed technique has been evaluated for several frequencies and multi-probe configurations. The use of a square array of probes has been proposed to distribute the measurement time savings over the vertical and horizontal dimensions. Nevertheless, other array configurations could be implemented (linear or rectangular), by treating the vertical and horizontal dimensions as two independent optimization problems.

Preliminary simulations of the method show good numerical stability against noisy data and drastic reductions in the number of samples. This reductions become more apparent for electrically large AUTs and measurement planes, where traditional measurements require thousands of samples.

Future work consists in the validation of the method with antenna measurement examples in a planar multi-probe set up. This would help to quantify the reductions on measurement time on real scenarios. In addition, the robustness of the method against probe pattern imbalances and other non ideal effects need to be analyzed.

Acknowledgement

This work was supported by Microwave Vision Group, by the Spanish Government, Ministry of Economy, National Program of Research, Development and Innovation under the project New Array Antenna Technologies and Digital Processing for the FUTURE Integrated Terrestrial and Space-based Millimeter Wave Radio Systems - UPM-InTerSpaCE (PID2020-112545RB-C51), and by the project TED2021-131975A-I00 /AEI/10.13039/501100011033/ Unión Europea NextGenerationEU/PRTR (ANTHEM5G).

References

[1] "IEEE Recommended Practice for Near-Field Antenna Measurements", in *IEEE Std 1720-2012*, pp.1-102, 5 Dec. 2012.

[2] "IEEE Standard Test Procedures for Antennas", in *ANSI-IEEE Std 149-1979*, vol., no., pp.1-144, 30 Nov. 1979

[3] S. F. Gregson, J. McCormick, and C. G. Parini, *Principles of Planar Near-Field Antenna Measurements*, The Institution of Engineering and Technology, London, UK, 2007.

[4] R. Johnson, H. Ecker, and R. Moore, "Compact range techniques and measurements," *IEEE Transactions on Antennas and Propagation*, vol. 17, no. 5, pp. 568–576, 1969.

[5] J. E. Hansen, *Spherical near-field antenna measurements*. IET, London, 1988.

[6] F. Rodríguez Varela et al, "Multi-Probe Measurement System Based on Single-Cut Transformation for Fast Testing of Linear Arrays", *Sensors*, 2021, 21, 1744.

[7] F. Saccardi et al., "Analysis of Probe Compensation Techniques for Fast Multi-Probe Planar Near Field Measurements," *2021 Antenna Measurement Techniques Association Symposium (AMTA)*, Daytona Beach, FL, USA, 2021, pp. 1-6.

[8] F. Saccardi et al., "Fast Multi-Probe Planar Near Field Measurements With Full Probe Compensation," *2021 15th European Conference on Antennas and Propagation (EuCAP)*, Dusseldorf, Germany, 2021, pp. 1-5.

[9] O. M. Bucci, C. Gennarelli and C. Savarese, "Representation of electromagnetic fields over arbitrary surfaces by a finite and nonredundant number of samples," in *IEEE Transactions on Antennas and Propagation*, vol. 46, no. 3, pp. 351-359, March 1998.

[10] O. Bucci and G. Franceschetti, "On the spatial bandwidth of scattered fields," in *IEEE Transactions on Antennas and Propagation*, vol. 35, no. 12, pp. 1445-1455, December 1987.

[11] N. Caccioppoli, C. Gennarelli, G. Riccio and C. Savarese, "The planar wide-mesh grid: an effective scanning for far-field reconstruction," *2005 IEEE Antennas and Propagation Society International Symposium, Washington*, DC, USA, 2005, pp. 412-415 vol. 3A.
bibitembib1001 F. Ferrara, C. Gennarelli, R. Guerriero, G. Riccio and C. Savarese, "An efficient near-field to far-field transformation using the planar wide-mesh scanning", *Journal of Electromagnetic Waves and Applications*, vol. 21, no. 3, pp. 341-357, 2007.

[12] F. D'Agostino, I. De Colibus, F. Ferrara, C. Gennarelli, R. Guerriero and M. Migliozzi, "Far-field pattern reconstruction from near-field data collected via a nonconventional plane-rectangular scanning: experimental testing", *International Journal of Antennas and Propagation*, vol. 2014, pp. 1-9, 2014.

[13] M. A. Saporetti et al., "Experimental Validation of Minimum Redundancy Scanning Schemes in PNF Measurements at V band," *2019 Antenna Measurement Techniques Association Symposium (AMTA)*, San Diego, CA, USA, 2019.

[14] N. Mézières, M. Mattes and B. Fuchs, "Antenna Characterization From a Small Number of Far-Field Measurements via Reduced-Order Models", in *IEEE Transactions on Antennas and Propagation*, vol. 70, no. 4, pp. 2422-2430, April 2022.

[15] Capozzoli A, Curcio C, Liseno A. "Different Metrics for Singular Value Optimization in Near-Field Antenna Characterization". *Sensors*, 2021, 21(6), 2122.

[16] A. Capozzoli, C. Curcio and A. Liseno, "Optimized spherical near-field antenna measurements," *The 8th European Conference on Antennas and Propagation (EuCAP)*, The Hague, Netherlands, 2014, pp. 1685-1689.

[17] A. Capozzoli, C. Curcio and A. Liseno, "Truncation in "Quasi-Raster" Near-Field Acquisitions [Measurements Corner]," in *IEEE Antennas and Propagation Magazine*, vol. 54, no. 5, pp. 174-183, Oct. 2012.

[18] A. Capozzoli, C. Curcio and A. Liseno, "Singular Value Optimization in Inverse Electromagnetic Scattering", in *IEEE Antennas and Wireless Propagation Letters*, vol. 16, pp. 1094-1097, 2017.

[19] R. Cornelius and D. Heberling, "Analysis of sampling grids for spherical near-field antenna measurements," in *Progress in Electromagnetics Research Symposium (PIERS)*, 2015, pp. 923–927.

[20] *https://www.mvg-world.com/en/products/antenna-measurement/hybrid-systems/t-dualscan*

[21] J. Fernandez Alvarez, J. M. Bjørstorp, O. Breinbjerg, "Spherical Phaseless Probe-Corrected Near-Field Measurements of the DTU-ESA VAST12 Reflector Antenna", *Proceedings of the 40th Annual Symposium of the Antenna Measurement Techniques Association*, 2018.

[22] S. Pivnenko et al., "Comparison of antenna measurement facilities with the DTU-ESA 12 GHz validation standard antenna within the EU antenna centre of excellence", *IEEE Transactions on Antennas Propagation*, vol. 57, no. 7, pp. 1863-1878, Jul. 2009.

[23] C. Cappellin, A. Frandsen and O. Breinbjerg, "Application of the SWE-to-PWE antenna diagnostics technique to an offset reflector antenna", *IEEE Antennas and Propagation Magazine*, vol. 50, no. 5, pp. 204-213, Oct. 2008

[24] F. Rodríguez Varela, B. G. Iragüen and M. Sierra-Castañer, "Application of Nonuniform FFT to Spherical Near-Field Antenna Measurements," in *IEEE Transactions on Antennas and Propagation*, vol. 68, no. 11, pp. 7571-7579, Nov. 2020.